



Distinct dynamic functional connectivity patterns of pain and touch thresholds: A resting-state fMRI study

Yueming Yuan^{a,b}, Li Zhang^{a,b}, Linling Li^{a,b}, Gan Huang^{a,b}, Ahmed Anter^{a,b}, Zhen Liang^{a,b}, Zhiguo Zhang^{a,b,c,*}

^a School of Biomedical Engineering, Health Science Center, Shenzhen University, Shenzhen, 518060, China

^b Guangdong Provincial Key Laboratory of Biomedical Measurements and Ultrasound Imaging, Shenzhen, 518060, China

^c Peng Cheng Laboratory, Shenzhen, 518055, China

ARTICLE INFO

Keywords:

Functional magnetic resonance imaging
Dynamic functional connectivity
Pain sensitivity
Pain threshold
Touch threshold

ABSTRACT

Dynamic functional connectivity (dFC) analysis based on resting-state functional magnetic resonance imaging (fMRI) has gained popularity in recent years. Despite many studies have linked dFC patterns to various mental diseases and cognitive functions, little research has used dFC in the investigation of low-level sensory perception. The present study is aimed to explore resting-state fMRI dFC patterns correlated with thresholds of two types of perception, pain and touch, on an individual basis. We collected and analyzed resting-state fMRI data and thresholds of pain and touch from 80 healthy participants. dFC states were identified by using independent component analysis, sliding window correlation, and clustering, and then the thresholds of pain and touch are correlated with the occurrence frequencies of dFC states. A new permutation analysis is developed to make identified dFC states more interpretable. We found that the occurrence frequency of a default mode network (DMN)-dominated state was positively correlated with the pain threshold, while the occurrence frequency of a static functional connectivity (sFC)-like state was negatively correlated with the touch threshold. This study showed that the thresholds of pain and touch have distinct dFC correlates, suggesting different influences of baseline brain states on different types of sensory perception. This study also showed that dFC could serve as an indicator of an individual's pain sensitivity, which can be potentially used for pain management.

1. Introduction

Inferring functional brain connectivity from resting-state functional magnetic resonance imaging (fMRI) has gained enormous popularity in the past decade [1]. Functional connectivity (FC) is generally estimated from statistical relationship between fMRI blood oxygen level dependent (BOLD) signals of different brain regions and it is most commonly calculated as the correlation coefficient between two BOLD signals in the whole scan [2,3]. However, this static FC (sFC) does not consider fluctuation in the relationship between BOLD signals [4–6], while there is much evidence (for example, from electrophysiological studies) showing that the FC has obvious dynamic behaviors even at rest [7]. Therefore, dynamic FC (dFC) has attracted increasing attention in recent years as a useful tool to probe the time-evolving organization of the brain.

The most popular method used to estimate dFC is the sliding window analysis [8], which splits the whole fMRI scan into a series of data segments and calculates time-dependent correlation for each

segment. Correlation can be calculated between fMRI signals of different brain regions or between components decomposed by using independent component analysis (ICA) on fMRI signals, resulting in a set of time-dependent correlation matrices. Next, clustering methods, such as k-means, are often used to group time-dependent correlation matrices of all time points and all participants into a limited number of dFC states with consistent spatial connectivity patterns. Subsequently, some dFC features, such as occurrence frequency and mean dwell time, can be extracted from these states. These dFC features can then be correlated with behavioral, cognitive, and pathological variables [9] in order to reveal neural correlates of cognition and mental disorders from resting-state fMRI. For example, many clinical studies have shown that dFC analysis reveals more information about the brain network than the traditional static FC analysis in many mental disorders, such as bipolar disorder, schizophrenia, autism spectrum disorder and mild cognitive impairment [10–13].

Generally, dFC is considered to measure the brain network's flexibility and adaptability, which are known to be essential in high-level

* Corresponding author at: School of Biomedical Engineering, Health Science Center, Shenzhen University, Shenzhen, China.

E-mail address: zgzhang@szu.edu.cn (Z. Zhang).

<https://doi.org/10.1016/j.bbr.2019.112142>

Received 13 May 2019; Received in revised form 7 July 2019; Accepted 2 August 2019

Available online 05 August 2019

0166-4328/ © 2019 Elsevier B.V. All rights reserved.

cognition and learning. For example, Yang et al. proved that the duration spent in connectivity states of a posteromedial cortex seed modulates mental flexibility [14]. Madhyastha et al. showed that stronger contributions of a dorsal attention subnetwork at rest lead to better attentional task performance [15]. Cohen reviewed how differences in dFC variability between different contexts relate to cognitive demands and behavioral performance and how different patterns of dFC correspond to individual differences in cognition [16]. But, dFC has been seldom linked to an individual's low-level sensory perception. Actually, sensory perception is influenced by high-level brain functions through top-down modulation, so it should be naturally regulated by the brain network's adaptability to environment and stimulation. For example, Cheng et al. demonstrated that patterns in dynamic and static brain communication were related to different characteristics and timescales of chronic pain using multivariate machine learning [17]. Bosma et al. proved that patients with multiple sclerosis have abnormal sFC, dFC and disrupted regional BOLD variability in the dynamic pain connectome [18]. Moreover, Hua et al. compared brain activations produced by pleasant, neutral and unpleasant touch, to the anterior lateral surface of lower leg of human subjects [19]. Therefore, it is reasonable to hypothesize that an individual's perception level (like pain and touch) is reflected in his/her dFC patterns.

In this study, we explore possible dFC correlates of two types of sensory perception: pain and touch. Specifically, we examined whether the perceived level of noxious stimuli (i.e., pain threshold) and the perceived level of non-noxious stimuli (i.e., touch threshold) are correlated with any dFC patterns on an individual basis. Pain is individualized sensory and emotional experience [20], and different people have different levels of pain sensitivity, which can be measured by pain thresholds in well-designed experiments. In recent years, many pain studies have used MRI/fMRI to find neural correlates of pain sensitivity. For example, it has been reported that individuals with high pain sensitivity have less gray matter in the precuneus and posterior cingulate cortex (PCC) [21]. However, it remains unknown whether an individual's pain sensitivity is related to dFC. It will also be very interesting to examine whether pain threshold and touch threshold, which respectively indicate an individual's sensitivity to nociceptive and non-nociceptive stimuli, have the same dFC correlates and underlying neurophysiological mechanisms.

To this end, we collected resting-state fMRI data and behavioral data (pain/touch thresholds) from 80 healthy participants. The sensations of touch and pain were respectively evoked by mechanical pressure and laser stimuli, and their thresholds were determined by participants' self-report. We used a dFC analysis framework to assess the reoccurred dynamic characteristics of FC, and the dFC analysis framework includes spatial-level group ICA to define brain networks of this group of participants, sliding window analysis to estimate dFC, and k-means clustering to estimate discrete dFC states. The basic idea of ICA is to separate underlying components that have been mixed together based on the assumption of independence of sources [22]. ICA has been popularly applied on fMRI data to isolate spatially independent components, each of which is represented as a set of brain regions sharing the same response pattern [22]. Group ICA is an ICA variant developed for the analysis of multisubject fMRI data and it can decompose multisubject resting-state fMRI data into functionally homogeneous regions [23,24]. Group ICA enables a whole-brain analysis for multiple subjects without resorting to atlas-based ROI analysis methods which may merge distinct areas [25] or fail to capture inter-subject spatial variability [26]. Next, dFC state features, such as occurrence frequency, were extracted and further correlated with the thresholds of pain and touch. To increase the interpretability of dFC states, we used the permutation analysis to quantify differences of dFC states and find dominant networks in each dFC state. By using above dFC analysis pipeline, we identified distinct dFC patterns for pain threshold and touch threshold, suggesting different baseline neural correlates of these two types of sensory perception.

2. Materials and Methods

2.1. Experimental design

A total of 80 healthy participants (32 males, 48 females, age: 22.11 ± 4.54 years) were recruited in this experiment. All participants were free of acute or chronic pain, nervous system diseases, cerebrovascular diseases, coronary heart disease and mental disorders. All participants gave their written informed consent and the experimental procedures were approved by the local ethics committee. The imaging data were scanned using a 3.0 T GE-scanner. Resting-state fMRI data was collected using a standard gradient echo planar imaging sequence with following imaging parameters: 43 oblique slices, thickness/gap = 3/0 mm, acquisition matrix = 64×64 , time of repetition (TR) = 2000 ms, time of echo (TE) = 30 ms, flip angle = 90° , field of view = 192×192 mm², total volume = 300, acquisition time = 10 min. In the whole scan, participants were asked to remain motionless, keep their eyes open, stay awake, relax their minds, and stare at the "+" sign with head fixation. However, due to the failure of data collection and head motion with more than 2.0 mm maximum displacement in any direction of x, y, and z or 2° of any angular motion throughout the scan [27–29], five participants were excluded and only data from the remaining 75 healthy participants (28 males, 47 females, age: 22.25 ± 4.64 years) were used in the subsequent analysis.

The thresholds of sensory perception were collected by two behavioral experiments. First, the touch threshold was measured manually by using a set of von Frey filament (0.008 g–300 g, corresponding to 0.08 mN – 2940 mN) to generate different strengths of transient mechanical pressure. The filament was touched vertically onto the back area of left hand until slightly bent. Each touch stimulus had a duration about 1 s and three consecutive stimuli were delivered in about 10 s. The transient pressure was given in an ascending order (starting from 0.008 g filament) and the participants were asked to report their feeling after each stimulus. When "feeling touch" was reported in any one of three consecutive stimuli, the corresponding pressure strength was recorded as the touch threshold. The result was averaged from two independent measurements conducted in one hour. Second, the pain threshold was measured manually by using laser equipment. Specifically, a series of laser stimuli were delivered to the back area between thumb and index finger of left hand. The measurement was started from energy level at 1 J with a 0.25 J increase at each stimulation. A participant was asked to report the pain ratings after each stimulation from 0 (no pain) to 10 (the worst pain). When a rating of 4 was reported, the corresponding energy level was recorded as the pain threshold. The result was averaged from two independent measurements conducted in one hour.

2.2. fMRI data preprocessing

All data processing processes were carried out in MATLAB-R2017a (The MathWorks, Inc., Natick, MA, US). The T1 weighted and resting-state fMRI data were preprocessed using the SPM8 (<https://www.fil.ion.ucl.ac.uk/spm>) and DPABI (<http://rfmri.org/dpabi>) [30]. The preprocessing procedure was as follows. The first 5 volumes were removed, remaining 295 volumes, to avoid T1 equilibration effects. Slice timing correction used the middle slice as the reference. Head motion correction was then used to obtain the six-dimensional rigid body motion parameters. The T1 images was segmented and co-registered with functional images. Then, the images were spatially normalized into Montreal Neurological Institute space, resliced to $3 \text{ mm} \times 3 \text{ mm} \times 3 \text{ mm}$ voxels, and smoothed with an FWHM of 6 mm. Variance normalization was used to remove the remarkable between-subject difference in the magnitude of signals and it was achieved at each voxel by linearly detrending and conversion to z-score (subtracting the mean from each of the individual data points and dividing the result by the standard deviation).

2.3. Group ICA analysis

The preprocessed resting-state fMRI data were concatenated, and spatial-level group ICA was performed using GIFT4.0b (<http://mialab.mrn.org/software/gift>) toolbox. The data were decomposed into numbers of independent components (ICs), which were fMRI time-series and spatial-maps decomposed from fMRI data and used to construct spatially-independent functional brain networks. We set the number of ICs to 100 for a detailed functional network separation [31]. The infomax ICA algorithm was repeated 100 times in ICASSO and the best run was selected to ensure the estimation stability. After estimating the aggregate spatial maps, spatiotemporal regression back reconstruction was performed to obtain the subject specific spatial maps and time courses. Additional post-processing steps were performed on the time courses of selected ICs, and these post-processing steps included detrending linear, quadratic, and cubic trends, conducting multiple regressions of the 6 realignment parameters and their temporal derivatives [32], despiking detected outliers [33], and low-pass filtering with cut-off frequency of 0.15 Hz.

For the classification of intrinsic connectivity networks (ICNs), which expanded upon the concept of restingstate networks to include the set of large-scale functionally connected brain networks [34,35]. We identified the useful components and the noise components according to whether the main power of time courses was in the low-frequency range and whether the peak coordinates of spatial maps were located in the gray matter. Then, we assigned the components to corresponding ICNs according to the location of peak coordinates and their overlap with ICNs obtained by previous studies [36].

2.4. dFC state analysis

The sliding window analysis approach was used to divide ICs time courses into several short segments to estimate dFC. A 30 TR (60 s) window, created by convolving a rectangle with a Gaussian ($\sigma = 3$ TR) and a step of 1 TR were used, resulting in 265 windows or segments. The results with other window sizes from 40 s to 80 s (20/25/35/40 TR) were provided in Section 1 of the Supplementary Materials. In each window, Pearson's correlation coefficients were calculated between each pair of ICs time courses. The correlation coefficient matrix had a dimension of $43 \times 43 \times 265$, where 43 was the number of retained ICs and 265 was the number of windows. Due to the symmetry of the correlation matrix, the subsequent analysis only used the upper triangle of the matrices at each time point.

Next, k-means clustering could be used to group the time-dependent FC matrices into a limited number of clusters, which are referred to as "states" in dFC analysis. The centers of states represent recurring FC patterns, and dFC features, such as the occurrence frequency of each state, could then be extracted. More precisely, the dFC matrices of all participants were first concatenated for k-means at the group-level. Then, the k-means was achieved in two steps. In the first step, the initial points of k-means were randomly set, which was repeated 100 times, and the result with the lowest within-cluster sums of point-to-centroid distances was retained. In the second step, the initial points were set as the centroids of the first-step k-means so that the adverse impact of small fluctuations can be avoided. The iteration number of k-means was set to 1000 to ensure the convergence. The optimal number of clusters (i.e., the number of dFC states) was determined by the elbow method, which calculates the ratio between inter-class distance and intra-class distance [37]. In the present study, the number of states was set to 4 by using the elbow method, and the details could be found in Section 2 of Supplementary Materials. After 4 dFC states were identified, the occurrence frequency of each state was obtained by calculating the percentage of the corresponding state among all time points for each participant. Because some subjects did not have some certain states (23 subjects did not have state 1, 46 subjects did not have state 2, 2 subjects did not have state 3, and 1 subject did not have state 4), the occurrence

frequency of subjects who had at least one window assigned to that state was used in subsequent correlation analysis.

2.5. Permutation analysis for characterizing dFC states

To further elucidate the differences between dFC states at the network (ICNs) level, we conducted a permutation test on dFC states. Because there are 7 ICNs, we have 28 network-pairs between these 7 ICNs: 7 within-network pairs and 21 between-network pairs. We averaged the FC value in each network-pair to obtain a 7×7 dFC state matrix at the level of networks for each participant. Then, the network-level FC matrices of all participants were randomly divided into four clusters with the same proportion as the actual k-means results (state1: 38%, state2: 13%, state3: 36%, state4: 33%) so that we obtained four randomly clustered dFC states. The random k-means clustering (permutation) process was repeated for 10,000 times. We calculated the difference of FC values between any two network-level dFC states in each permutation, and generated a probability density function of FC difference between any two states at each network-pair. The actual FC differences between two states were located in the permutation-based probability density functions to obtain their significance levels (p-values). If one state had a significantly higher FC than another state at one network-pair, this state had a strength ranking score of 1 at this network-pair. So, each network-pair of each state has a strength ranking score from 0 to 3. For example, if one state's FC is significantly higher than those of all other three states at one network-pair, this network-pair of this state has a strength ranking score of 3. By such a permutation analysis and sorting of FC for each network-pair, we could determine the distinct network-level FC values for each state so that a better characterization of dFC states can be achieved. In addition, to check the correlation between dFC states and sFC, we also calculated the Pearson's correlation coefficients between each dFC state and sFC.

2.6. Correlation and decorrelation analyses

Next, we calculated the Pearson's correlation coefficients between the dFC features and the thresholds of pain and touch with covariates including age, gender and head motion (framework displacement [33]). Because there are 8 correlations (2 thresholds \times 4 states feature), false discovery rate (FDR) was used to correct the problem of multiple comparisons. Furthermore, because pain threshold and touch threshold were significantly correlated, these thresholds were decorrelated using principal component analysis (PCA), resulting in two decorrelated eigenvectors (PC1 and PC2). The Pearson's correlation coefficients between two decorrelated eigenvectors and the features of four states were calculated as well.

3. Results

3.1. Group ICA components

By using group ICA and selecting ICs, we retained 43 of the 100 ICs that make up seven ICNs: sub-cortical network (SCN), auditory network (AND), somatomotor network (SMN), visual network (VSN), cognitive control network (CCN), default mode network (DMN) and cerebellar network (CBN). The SCN contained 5 ICs, mainly located in putamen and thalamus. The ADN had 1 ICs, located in the temporal region. The SMN contained 10 ICs, mainly located in precentral, postcentral and supplementary motor areas. The VSN contained 9 ICs, mainly located in occipital regions, fusiform and cuneus. The CCN contained 10 ICs, mainly located in the frontal lobe and insula. The DMN contained 7 ICs, mainly located in precuneus and frontal lobes. The CBN had 1 ICs located in cerebellum region. The ICs and the ICNs could be seen in Fig. 1, and the specific location and distribution of each ICs could be found in Section 3 of Supplementary Materials.

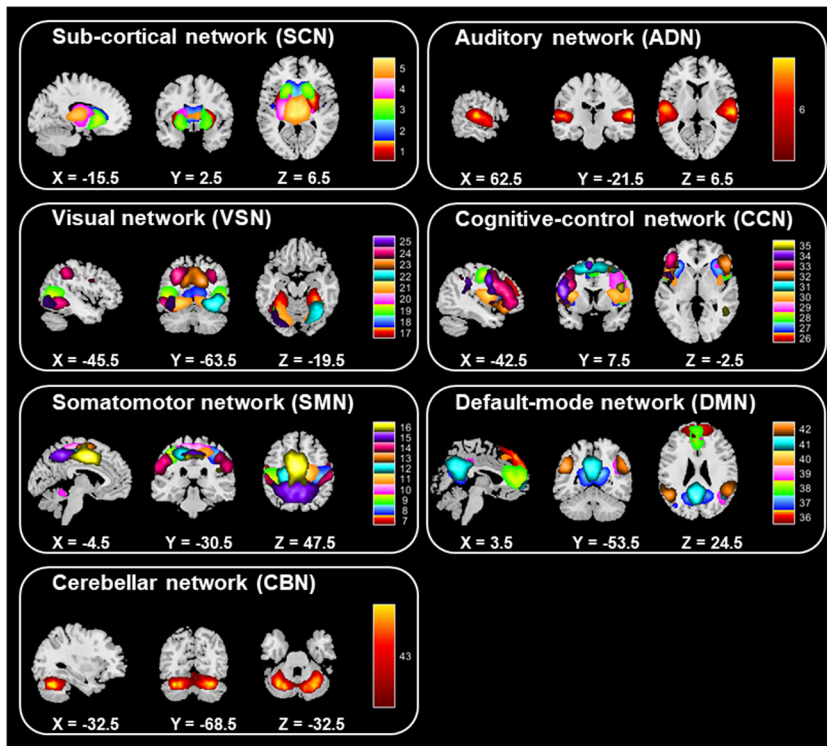


Fig. 1. The ICs spatial map. 43 ICs were grouped into 7 ICNs. There were 5 ICs in the sub-cortical network (SCN), 1 ICs in the auditory network (ADN), 9 ICs in the visual network (VSN), 10 ICs in the cognitive control network (CCN), 10 ICs in the somatomotor network (SMN), 7 ICs in the default mode network (DMN), and 1 ICs in the cerebellar network (CBN).

3.2. dFC states

Through the sliding window method and k-means, 4 dFC states were recognized, which were shown as the group-level k-means centroids in Fig. 2. The results showed that state 1 accounted for 38%, state 2 accounted for 13%, state 3 accounted for 16% and state 4 accounted for 33%. However, the proportion of time occupied by various dFC states (i.e., the occurrence frequency) in different participant was different. For comparison, sFC estimated from the whole fMRI scan was also showed in Fig. 2.

3.3. Characterizations of dFC states

We used permutation analysis to further explore the differences between dFC states at the network level. The results were showed in Fig. 3, which indicated that states 2 and 3 generally had stronger FC than states 1 and 4 in almost all network-pairs. The strongest FC in state 2 was concentrated in SCN, ADN and SMN, while the strongest FC in state 3 was concentrated in DMN. Therefore, state 3 is referred to as a DMN-dominated state hereinafter. Moreover, we calculated the correlations between dFC states and sFC. The results showed state 4 was most correlated with sFC ($R = 0.93, p < 0.001$), while other states were also correlated with sFC (state 1: $R = 0.92, p < 0.001$; state 2:

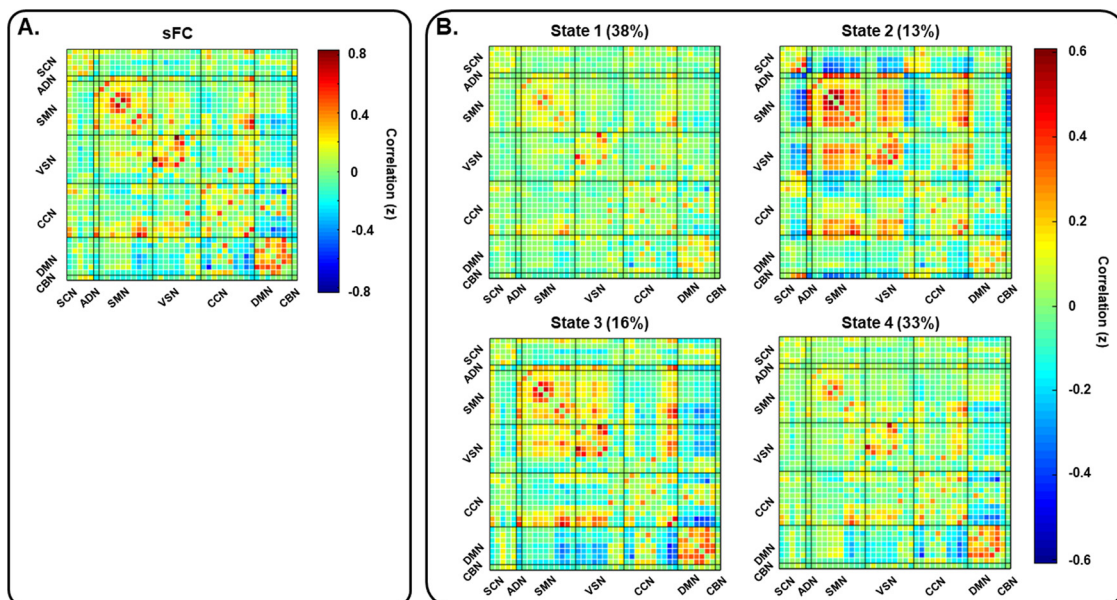


Fig. 2. A. The static FC (sFC) estimated from the whole fMRI scan. B. Four dFC states obtained by sliding window analysis and group-level k-means. The proportion of four states were 38%, 13%, 16% and 33%, respectively.

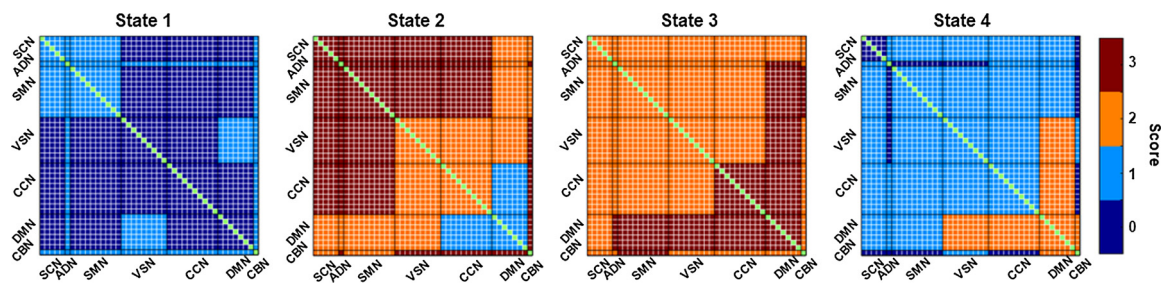


Fig. 3. Comparison of FC strength between four dFC states. Permutation test compared any two states at each network-pair to obtain the strength ranking score of FC strength for each network-pair. If one state had a significantly higher FC than another state at one network-pair, this state had a strength ranking score of 1 at this network-pair. So, each network-pair of each state has a strength ranking score from 0 to 3. For example, if one state's FC is significantly higher than those of all other three states at one network-pair, this network-pair of this state has a strength ranking score of 3.

$R = 0.77, p < 0.001$; state 3: $R = 0.88, p < 0.001$). Therefore, state 4 is referred to as a sFC-like state hereinafter. From the above results, we could know the differences between four dFC states and their dominant network-pairs, which provided a better characterization and interpretation of dFC states.

3.4. Correlations and decorrelation analyses

The correlations between pain or touch thresholds and occurrence frequencies of states were showed in Fig. 4. We found that the occurrence frequency of state 3 was significantly positively correlated with the pain threshold ($R = 0.36, p = 0.002, p_{FDR} = 0.008$), but not significantly correlated with the touch threshold ($R = 0.10, p = 0.406, p_{FDR} = 0.008$). On the other hand, the occurrence frequency of state 4 was significantly negatively correlated with the touch threshold ($R = -0.34, p = 0.003, p_{FDR} = 0.008$), but not significantly correlated with the pain threshold ($R = -0.18, p = 0.118, p_{FDR} = 0.008$).

We further found that there was a positive correlation between pain threshold and touch threshold ($R = 0.24, p = 0.038$). We used PCA to decompose pain and touch thresholds into two decorrelated eigenvectors. The correlations between decorrelated eigenvectors and occurrence frequencies of dFC states were shown in Fig. 5. The occurrence

frequency of state 3 was significantly positively correlated with PC1 ($R = 0.35, p = 0.002, p_{FDR} = 0.019$) but not significantly correlated with PC2 ($R = -0.03, p = 0.792, p_{FDR} = 0.019$). The occurrence frequency of state 4 was significantly negatively correlated with PC1 ($R = -0.28, p = 0.016, p_{FDR} = 0.019$) but not significantly correlated with PC2 ($R = -0.25, p = 0.031, p_{FDR} = 0.019$).

4. Discussion

In the present study, we investigated the correlation between dFC states and pain/touch thresholds on an individual basis. It was found that pain threshold and touch threshold are correlated with the occurrence frequency of different dFC states, suggesting different mechanisms underlying these two types of perception.

4.1. dFC correlates of sensory perception

dFC analysis has been popularly used in past several years as a new type of baseline neural correlates of behavioral and cognitive variables [14–16,38,39]. However, dFC is seldom adopted to study low-level sensory perception, which may be due to the following reasons. First, dFC is indicative of the brain network's flexibility and adaptability,

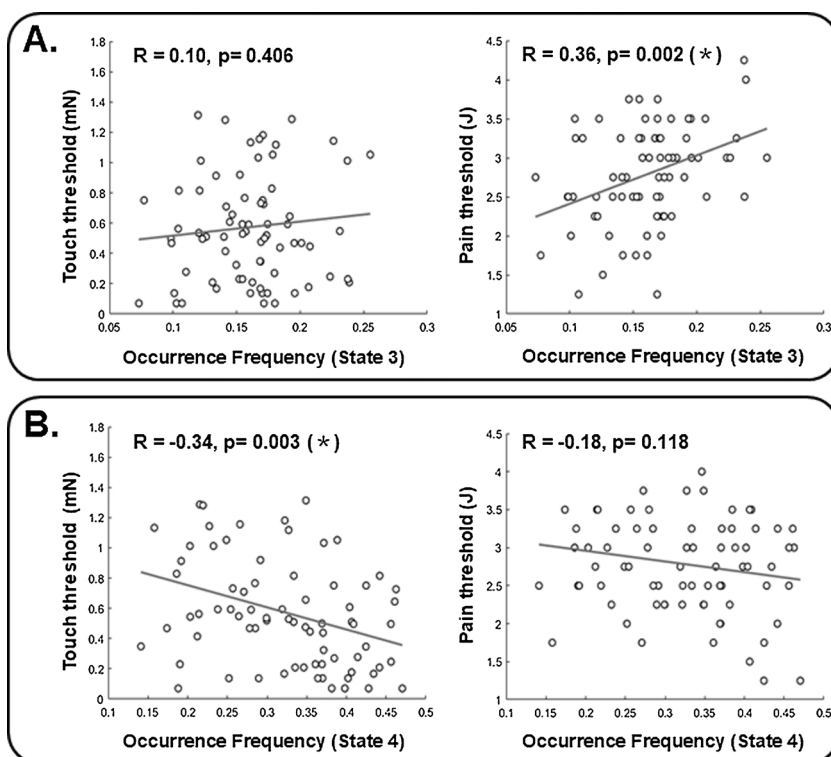


Fig. 4. Correlations between occurrence frequency of dFC states and pain/touch thresholds. Only the correlation results of state 3 and state 4 are shown here because these two states have significant correlations with pain/touch thresholds. A. The occurrence frequency of state 3 was not significantly correlated with touch threshold ($R = 0.10, p = 0.406$) but significantly correlated with pain threshold ($R = 0.36, p = 0.002$). B. The occurrence frequency of state 4 was significantly correlated with touch threshold ($R = -0.34, p = 0.003$) but not significantly correlated with pain threshold ($R = -0.18, p = 0.118$). Note that FDR-adjusted significance level is $p < 0.008$ and significant correlations are marked with *.

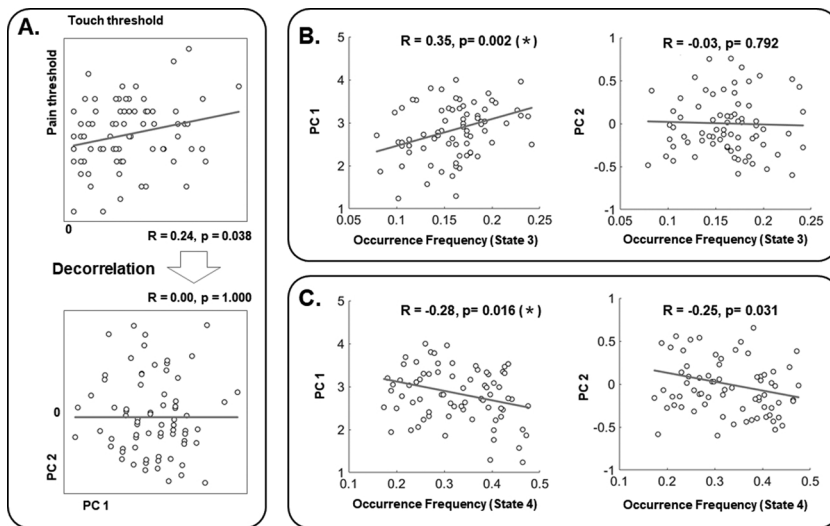


Fig. 5. Correlations between occurrence frequency of dFC states and decorrelated eigenvectors (PC1 and PC2) transformed from pain and touch thresholds using PCA. Only the correlation results of state 3 and state 4 are shown here because these two states have significant correlations with pain/touch thresholds. A. The correlation between pain threshold and touch threshold and two decorrelated eigenvectors PC1 and PC2. B. The occurrence frequency of state 3 was significantly positively correlated with PC1 ($R = 0.35$, $p = 0.002$) but not significantly correlated with PC2 ($R = -0.03$, $p = 0.792$). C. The occurrence frequency of state 4 was significantly negatively correlated with PC1 ($R = -0.28$, $p = 0.016$) but not significantly correlated with PC2 ($R = -0.25$, $p = 0.031$). Note that FDR-adjusted significance level is $p < 0.019$, and significant correlations are marked with *.

which are generally believed to be related to high-level cognitive activities because cognition needs large-scale re-organization of brain networks. Second, sensory perception is more often studied at a trial-by-trial level (i.e., to study responses to multiple trials of stimuli delivered to one individual), but dFC is estimated on an individual basis.

In this study, we hypothesized that an individual's perception level is correlated with dFC and this hypothesis was developed based on three lines of reasoning. First, low-level sensory perception is modulated by high-level brain functions through top-down modulation. So, perception should also be related to dFC patterns, which are closely related to high-level cognition, at least in an indirect manner. Second, the brain keeps organizing its connections to adapt to changes in external environment, which obviously include delivery of sensory stimuli. Therefore, as an indicator of the level of dynamic organization of the brain, dFC may also be able to modulate an individual's perception level. Third, many previous studies have revealed that, fluctuations of brain networks modulate the brain responses and perception to forthcoming sensory stimuli on a trial-by-trial basis. In another word, pre-stimulus brain networks predict the perception level in response to a sensory stimulus (such as visual stimulation [40], somatosensory stimulation [41], pain stimulation [42]). Hence, we speculated that, such a relationship between FC fluctuations and sensory perception can also be observed on an individual basis.

This hypothesis was supported by our experimental results, indicating that the occurrence frequency of certain dFC states is related to the overall perception level of pain or touch. These results suggest that, dFC, as a window to probe the brain's adaptability, does not only modulate high-level cognition, but also determines low-level sensory perception on an individual level.

4.2. Distinct dFC correlates of pain and touch thresholds

Pain and touch are perceived via different receptors in the skin, but their activations in the brain are largely overlapped [43]. Therefore, to find pain-specific brain activation patterns has been a central topic in the research of pain neuroimaging [44–46]. This study showed that, on an individual level, pain and touch have different dFC correlates, implying their different neural basis. According to our results, the occurrence frequency of dFC state 3, which was mainly dominated by DMN, was significantly positively related to the pain threshold. This state 3 showed strong positive connectivity within DMN and negative connectivity between DMN and other networks. The role of DMN has been well documented in literature, and it could play an important role in attention, expectation, vigilance, memory, and so on [47–49]. The role of DMN in pain perception has also been well studied, mainly by

checking the sFC on an individual level or pre-stimulus FC on a trial-by-trial level. For example, Alshelh et al. reported disruption of DMN dynamics in acute and chronic pain states [50]. Our previous work also showed the pre-stimulus fMRI signals in the DMN negatively predicted the perceived intensity of subsequent painful stimuli [51]. This study revealed the role of DMN in pain from another aspect: the occurrence frequency of a DMN-dominated dFC state is positively related to the overall level of pain perception. This may suggest that, if an individual has more frequent DMN connections at rest, which may be indicative of higher vigilance or attention, his/her sensitivity to pain is lower.

On the other hand, the touch threshold is not correlated with the DMN-dominated state 3, but it is related to a sFC-like dFC state 4. The occurrence frequency of state 4 is negatively correlated with touch threshold, implying that if the sFC-like state 4 appears more frequently, the individual has a smaller touch threshold. Because state 4 is similar to sFC, the occurrence frequency of state 4 could be indicative of the stability or stationarity of FC. These suggest that, if an individual has less fluctuant FC at rest, the individual sensitivity to touch is higher.

Because touch threshold and pain threshold were correlated, they might share some common behavioral characteristics and underlying neural mechanisms. By using PCA to decompose two thresholds into two orthogonal components, we found that the main component, PC1, is significantly positively correlated with the occurrence frequency of state 3 and significantly negatively correlated with the occurrence frequency of state 4. Hence, PC1 should be the common behavioral characteristics of pain and touch thresholds, and it is modulated by both the DMN-dominated state 3 and the sFC-like state 4. On the other hand, PC2 is correlated with neither the occurrence frequency of state 3 nor the occurrence frequency of state 4. We speculate that PC2 explains the different behavioral characteristics of pain and touch thresholds and it is not correlated with dFC features. Since touch and pain thresholds are different linear combinations of PC1 and PC2, these two thresholds exhibit different correlations with dFC features.

4.3. Limitations and future work

In the present study, dFC was estimated using a sliding window size of $TR = 30$ (60 s). Wilson et al. proved that a time window between 30 and 100 s is a comparatively good window length for dFC [52], and Shirer et al. demonstrated that cognitive states may be correctly identified from covariance matrices estimated on as little as 30 – 60 s of data [25]. Therefore, we selected a window size of 60 s in the present study. We also examined the results with other window sizes (40 s, 50 s, 70 s, and 80 s), and we found that the dFC analysis results remained stable for window sizes between 50 s and 70 s. Results with other

window sizes were provided in Section 1 of the Supplementary Materials. Furthermore, the number of states was determined using the elbow criterion of the cluster validity index, which was computed as the ratio between within-cluster distance to between-cluster distance. We also provided clustering results of $k = 3$ to 5 in Section 2 of the Supplementary Materials. These results demonstrated that $k = 4$ can obtain four stable states, while $k = 3$ could merge distinct dFC states and $k = 5$ could generate redundant states.

We only found one dFC feature was associated with sensory perception thresholds and the correlation coefficient was about 0.35. The correlation is not large, which may due to the small number of subjects ($N = 75$). We checked some recent related papers and found that significant but small (for example, $R < 0.4$) correlations between dFC features and behavioral or cognitive parameters were commonly reported [53–55]. In our study, because the significant correlations passed a strict significance level (FDR corrected 0.05), we believed that the significant correlations found in this study were meaningful. We also calculated the correlation between pain/touch thresholds and another dFC feature, mean dwell time, but no correlation could pass the significance level.

One limitation of this study was the fact that it was only focused on pressure touch and laser-evoked pain, but it should certainly be extended to other sensory modalities (visual, auditory, etc.) and other pain stimulation modalities (cold pain, electricity-evoked pain, etc.). It will be interesting to check the common and specific dFC patterns in modulating the perception levels of different sensory modalities and pain stimulation.

As for future work, the rapid developments of dFC analysis pipelines and methods enable extraction of more meaningful information from dynamic patterns of FC. For example, by using fuzzy meta-state analysis on time-varying coefficient coefficients, more dFC features can be estimated [56]. Hence, advanced dFC analysis frameworks may potentially reveal more dFC correlates of individualized levels of perception.

5. Conclusion

In the present study, we found that the occurrence frequency of a DMN-dominated dFC state was significantly correlated with an individual's pain threshold, while the occurrence frequency of a sFC-like dFC state was significantly correlated with an individual's touch threshold. These results suggest that dFC is a useful tool to investigate low-level sensory perception on an individual basis. The study also showed that dFC could also be an indicator of an individual's pain sensitivity, which could be potentially used for pain management in clinical uses.

Declaration of Competing Interest

None of the authors have potential conflicts of interest to be disclosed.

Acknowledgements

We thank Li Hu (Institute of Psychology, Chinese Academy Sciences), Meng Liang (Tianjin Medical University), Jixin Liu (Xidian University), and Yazhou Kong (Institute of Psychology, Chinese Academy Sciences) for jointly designing, planning, and conducting experiments. This work was supported by National Natural Science Foundation of China (No.81871443); Science, Technology and Innovation Commission of Shenzhen Municipality Technology Fund (No.JCYJ20170818093322718); and Shenzhen Peacock Plan (No.KQTD2016053112051497).

Appendix A. Supplementary data

Supplementary data associated with this article can be found, in the

online version, at <https://doi.org/10.1016/j.bbr.2019.112142>.

References

- [1] A.K. Azeez, B.B. Biswal, A review of resting-state analysis methods, *Neuroimaging Clin. N. Am.* 27 (4) (2017) 581–592, <https://doi.org/10.1016/j.nic.2017.06.001>.
- [2] M.D. Fox, M. Greicius, Clinical applications of resting-state functional connectivity, *Front. Syst. Neurosci.* 4 (2010) 19, <https://doi.org/10.3389/fnsys.2010.00019>.
- [3] M.D. Greicius, Resting-state functional connectivity in neuropsychiatric disorders, *Curr. Opin. Neurol.* 21 (4) (2008) 424–430, <https://doi.org/10.1097/WCO.0b013e328328306f2c5>.
- [4] R.M. Hutchison, T. Womelsdorf, E.A. Allen, et al., Dynamic functional connectivity: promise, issues, and interpretations, *Neuroimage* 80 (2013) 360–378, <https://doi.org/10.1016/j.neuroimage.2013.05.079>.
- [5] M.G. Preti, T.A. Bolton, D. Van De Ville, The dynamic functional connectome: state-of-the-art and perspectives, *Neuroimage* 160 (2017) 41–54, <https://doi.org/10.1016/j.neuroimage.2016.12.061>.
- [6] V.D. Calhoun, R. Miller, G. Pearlson, et al., The chronnectome: time-varying connectivity networks as the next frontier in fMRI data discovery, *Neuron* 84 (2) (2014) 262–274, <https://doi.org/10.1016/j.neuron.2014.10.015>.
- [7] S.D. Keilholz, The neural basis of time-varying resting-state functional connectivity, *Brain Connect.* 4 (10) (2014) 769–779, <https://doi.org/10.1089/brain.2014.0250>.
- [8] V. Kiviniemi, T. Vire, J. Remes, et al., A sliding time window ICA reveals spatial variability of the default mode network in time, *Brain Connect.* 1 (4) (2011) 339–347, <https://doi.org/10.1089/brain.2011.0036>.
- [9] B. Rashid, E. Damaraju, G.D. Pearlson, et al., Dynamic connectivity states estimated from resting fMRI Identify differences among Schizophrenia, bipolar disorder, and healthy control subjects, *Front. Hum. Neurosci.* 8 (2014) 897, <https://doi.org/10.3389/fnhum.2014.00897>.
- [10] Y. Du, G.D. Pearlson, D. Lin, et al., Identifying dynamic functional connectivity biomarkers using GIG-ICA: application to schizophrenia, schizoaffective disorder, and psychotic bipolar disorder, *Human Brain Mapp* 38 (5) (2017) 2683–2708, <https://doi.org/10.1002/hbm.23553>.
- [11] X. Chen, H. Zhang, Y. Gao, et al., High-order resting state functional connectivity network for MCI classification, *Hum. Brain Mapp.* 37 (9) (2016) 3282–3296, <https://doi.org/10.1002/hbm.23240>.
- [12] Q. Yu, E.B. Erhardt, J. Sui, et al., Assessing dynamic brain graphs of time-varying connectivity in fMRI data: application to healthy controls and patients with schizophrenia, *Neuroimage* 107 (2015) 345–355, <https://doi.org/10.1016/j.neuroimage.2014.12.020>.
- [13] C.Y. Wee, P.T. Yap, D. Shen, Diagnosis of autism spectrum disorders using temporally distinct resting-state functional connectivity networks, *CNS Neurosci. Ther.* 22 (3) (2016) 212–219, <https://doi.org/10.1111/cns.12499>.
- [14] Z. Yang, R.C. Craddock, D.S. Margulies, et al., Common intrinsic connectivity states among posteromedial cortex subdivisions: insights from analysis of temporal dynamics, *Neuroimage* 93 (Pt 1) (2014) 124–137, <https://doi.org/10.1016/j.neuroimage.2014.02.014>.
- [15] T.M. Madhyastha, M.K. Askren, P. Boord, et al., Dynamic connectivity at rest predicts attention task performance, *Brain Connect.* 5 (1) (2015) 45–59, <https://doi.org/10.1089/brain.2014.0248>.
- [16] J.R. Cohen, The behavioral and cognitive relevance of time-varying, dynamic changes in functional connectivity, *Neuroimage* 180 (Pt B) (2018) 515–525, <https://doi.org/10.1016/j.neuroimage.2017.09.036>.
- [17] J.C. Cheng, A. Rogachov, K.S. Hemington, et al., Multivariate machine learning distinguishes cross-network dynamic functional connectivity patterns in state and trait neuropathic pain, *Pain* 159 (9) (2018) 1764–1776, <https://doi.org/10.1097/j.pain.0000000000001264>.
- [18] R.L. Bosma, J.A. Kim, J.C. Cheng, et al., Dynamic pain connectome functional connectivity and oscillations reflect multiple sclerosis pain, *Pain* 159 (11) (2018) 2267–2276, <https://doi.org/10.1097/j.pain.0000000000001332>.
- [19] Q.P. Hua, X.Z. Zeng, J.Y. Liu, et al., Dynamic changes in brain activations and functional connectivity during affectively different tactile stimuli, *Cell. Mol. Neurobiol.* 28 (1) (2008) 57–70, <https://doi.org/10.1007/s10571-007-9228-z>.
- [20] D.D. Price, Psychological and neural mechanisms of the affective dimension of pain, *Science* 288 (5472) (2000) 1769–1772, <https://doi.org/10.1126/science.288.5472.1769>.
- [21] N.M. Emerson, F. Zeidan, O.V. Lobanov, et al., Pain sensitivity is inversely related to regional grey matter density in the brain, *Pain* 155 (3) (2014) 566–573, <https://doi.org/10.1016/j.pain.2013.12.004>.
- [22] V.D. Calhoun, T. Adali, G.D. Pearlson, et al., A method for making group inferences from functional MRI data using independent component analysis, *Hum. Brain Mapp.* 14 (3) (2001) 140–151, <https://doi.org/10.1002/hbm.1048>.
- [23] V. Kiviniemi, T. Starck, J. Remes, et al., Functional segmentation of the brain cortex using high model order group PICA, *Hum. Brain Mapp.* 30 (12) (2009) 3865–3886, <https://doi.org/10.1002/hbm.20813>.
- [24] A. Abou-Elseoud, T. Starck, J. Remes, et al., The effect of model order selection in group PICA, *Hum. Brain Mapp.* 31 (8) (2010) 1207–1216, <https://doi.org/10.1002/hbm.20929>.
- [25] W.R. Shirer, S. Ryali, E. Rykhlevskaia, et al., Decoding subject-driven cognitive states with whole-brain connectivity patterns, *Cereb. Cortex* 22 (1) (2012) 158–165, <https://doi.org/10.1093/cercor/bhr099>.
- [26] E.A. Allen, E.B. Erhardt, Y. Wei, et al., Capturing inter-subject variability with group independent component analysis of fMRI data: a simulation study, *Neuroimage* 59 (4) (2012) 4141–4159, <https://doi.org/10.1016/j.neuroimage.2011.10.010>.
- [27] Y. Chao-Gan, Z. Yu-Feng, DPARSF: a MATLAB toolbox for "Pipeline" data analysis of

- resting-state fMRI, *Front. Syst. Neurosci.* 4 (2010) 13, <https://doi.org/10.3389/fnsys.2010.00013>.
- [28] B.K. Yuan, J. Wang, Y.F. Zang, et al., Amplitude differences in high-frequency fMRI signals between eyes open and eyes closed resting states, *Front. Hum. Neurosci.* 8 (2014) 503, <https://doi.org/10.3389/fnhum.2014.00503>.
- [29] B. Yuan, Y. Fang, Z. Han, et al., Brain hubs in lesion models: predicting functional network topology with lesion patterns in patients, *Sci. Rep.* 7 (1) (2017) 17908, <https://doi.org/10.1038/s41598-017-17886-x>.
- [30] C.G. Yan, X.D. Wang, X.N. Zuo, et al., DPABI: data processing & analysis for (Resting-State) brain imaging, *Neuroinformatics* 14 (3) (2016) 339–351, <https://doi.org/10.1007/s12021-016-9299-4>.
- [31] E.A. Allen, E. Damaraju, S.M. Plis, et al., Tracking whole-brain connectivity dynamics in the resting-state, *Cereb. Cortex* 24 (3) (2014) 663–676, <https://doi.org/10.1093/cercor/bhs352>.
- [32] T.D. Satterthwaite, M.A. Elliott, R.T. Gerraty, et al., An improved framework for confound regression and filtering for control of motion artifact in the preprocessing of resting-state functional connectivity data, *Neuroimage* 64 (2013) 240–256, <https://doi.org/10.1016/j.neuroimage.2012.08.052>.
- [33] J.D. Power, A. Mitra, T.O. Laumann, et al., Methods to detect, characterize, and remove motion artifact in resting-state fMRI, *Neuroimage* 84 (2014) 320–341, <https://doi.org/10.1016/j.neuroimage.2013.08.048>.
- [34] A.R. Laird, P.M. Fox, S.B. Eickhoff, et al., Behavioral interpretations of intrinsic connectivity networks, *J. Cogn. Neurosci.* 23 (12) (2011) 4022–4037, https://doi.org/10.1162/jocn_a.00077.
- [35] W.W. Seeley, V. Menon, A.F. Schatzberg, et al., Dissociable intrinsic connectivity networks for salience processing and executive control, *J. Neurosci.* 27 (9) (2007) 2349–2356, <https://doi.org/10.1523/JNEUROSCI.5587-06.2007>.
- [36] Z. Fu, Y. Tu, X. Di, et al., Characterizing dynamic amplitude of low-frequency fluctuation and its relationship with dynamic functional connectivity: an application to schizophrenia, *Neuroimage* S53-8119 (17) (2017) 30783–30788, <https://doi.org/10.1016/j.neuroimage.2017.09.035>.
- [37] E. Damaraju, E.A. Allen, A. Belger, et al., Dynamic functional connectivity analysis reveals transient states of dysconnectivity in schizophrenia, *Neuroimage Clin.* 5 (2014) 298–308, <https://doi.org/10.1016/j.nicl.2014.07.003>.
- [38] R.P. Viviano, N. Raz, P. Yuan, et al., Associations between dynamic functional connectivity and age, metabolic risk, and cognitive performance, *Neurobiol. Aging* 59 (2017) 135–143, <https://doi.org/10.1016/j.neurobiolaging.2017.08.003>.
- [39] B.Y. Park, T. Moon, H. Park, Dynamic functional connectivity analysis reveals improved association between brain networks and eating behaviors compared to static analysis, *Behav. Brain Res.* 337 (2018) 114–121, <https://doi.org/10.1016/j.bbr.2017.10.001>.
- [40] S. Hanslmayr, A. Aslan, T. Staudigl, et al., Pre-stimulus oscillations predict visual perception performance between and within subjects, *Neuroimage* 37 (4) (2007) 1465–1473, <https://doi.org/10.1016/j.neuroimage.2007.07.011>.
- [41] M. Boly, E. Baetee, C. Schnakers, et al., Baseline brain activity fluctuations predict somatosensory perception in humans, *Proc Natl Acad Sci U S A* 104 (29) (2007) 12187–12192, <https://doi.org/10.1073/pnas.0611404104>.
- [42] Y. Tu, A. Tan, Y. Bai, et al., Decoding subjective intensity of nociceptive pain from pre-stimulus and post-stimulus brain activities, *Front. Comput. Neurosci.* 10 (2016) 32, <https://doi.org/10.3389/fncom.2016.00032>.
- [43] F. Lui, D. Duzzi, M. Corradini, et al., Touch or pain? Spatio-temporal patterns of cortical fMRI activity following brief mechanical stimuli, *Pain* 138 (2) (2008) 362–374, <https://doi.org/10.1016/j.pain.2008.01.010>.
- [44] M. Liang, A. Mouraux, L. Hu, et al., Primary sensory cortices contain distinguishable spatial patterns of activity for each sense, *Nat. Commun.* 4 (2013) 1979, <https://doi.org/10.1038/ncomms2979>.
- [45] J. Liu, H. Liu, J. Mu, et al., Altered white matter microarchitecture in the cingulum bundle in women with primary dysmenorrhea: a tract-based analysis study, *Hum. Brain Mapp.* 38 (9) (2017) 4430–4443, <https://doi.org/10.1002/hbm.23670>.
- [46] L. Hu, G.D. Iannetti, Neural indicators of perceptual variability of pain across species, *Proc. Natl. Acad. Sci. U. S. A.* 116 (5) (2019) 1782–1791, <https://doi.org/10.1073/pnas.1812499116>.
- [47] R.L. Buckner, J.R. Andrews-Hanna, D.L. Schacter, The brain's default network: anatomy, function, and relevance to disease, *Ann. N. Y. Acad. Sci.* 1124 (2008) 1–38, <https://doi.org/10.1196/annals.1440.011>.
- [48] D.T. Gilbert, T.D. Wilson, Propection: experiencing the future, *Science* 317 (5843) (2007) 1351–1354, <https://doi.org/10.1126/science.1144161>.
- [49] J.R. Andrews-Hanna, J.S. Reidler, J. Sepulcre, et al., Functional-anatomic fractionation of the brain's default network, *Neuron* 65 (4) (2010) 550–562, <https://doi.org/10.1016/j.neuron.2010.02.005>.
- [50] Z. Alshelh, K.K. Marciszewski, R. Akhter, et al., Disruption of default mode network dynamics in acute and chronic pain states, *Neuroimage Clin.* 17 (2017) 222–231, <https://doi.org/10.1016/j.nicl.2017.10.019>.
- [51] Y. Tu, Z. Zhang, A. Tan, et al., Alpha and gamma oscillation amplitudes synergistically predict the perception of forthcoming nociceptive stimuli, *Hum. Brain Mapp.* 37 (2) (2016) 501–514, <https://doi.org/10.1002/hbm.23048>.
- [52] R.S. Wilson, S.D. Mayhew, D.T. Rollings, et al., Influence of epoch length on measurement of dynamic functional connectivity in wakefulness and behavioural validation in sleep, *Neuroimage* 112 (2015) 169–179, <https://doi.org/10.1016/j.neuroimage.2015.02.061>.
- [53] L. Deng, Y. Cheng, X. Cao, et al., The effect of cognitive training on the brain's local connectivity organization in healthy older adults, *Sci. Rep.* 9 (1) (2019) 9033, <https://doi.org/10.1038/s41598-019-45463-x>.
- [54] S. Neufang, M.J. Geiger, G.A. Homola, et al., Cognitive-behavioral therapy effects on alerting network activity and effective connectivity in panic disorder, *Eur. Arch. Psychiatry Clin. Neurosci.* (2018) 1–12, <https://doi.org/10.1007/s00406-018-0945-8>.
- [55] N. Deris, C. Montag, M. Reuter, et al., Functional connectivity in the resting brain as biological correlate of the Affective Neuroscience Personality Scales, *Neuroimage* 147 (2017) 423–431, <https://doi.org/10.1016/j.neuroimage.2016.11.063>.
- [56] A. Abrol, E. Damaraju, R.L. Miller, et al., Replicability of time-varying connectivity patterns in large resting state fMRI samples, *Neuroimage* 163 (2017) 160–176, <https://doi.org/10.1016/j.neuroimage.2017.09.020>.